

## Masses of $^{52g}\text{Co}$ and $^{52m}\text{Co}$ and their impact on the $\beta$ -decay properties of $^{52}\text{Ni}^*$

Yu-Hu Zhang<sup>†</sup>

*on behalf of CSRe mass measurement collaboration,  
Key Laboratory of High Precision Nuclear Spectroscopy,  
Institute of Modern Physics, Chinese Academy of Sciences, Lanzhou 730000, China  
E-mail: yhzhang@impcas.ac.cn*

Mass excesses of  $^{52}\text{Co}$  and its ( $2^+$ ) isomer are measured to be  $-34361(8)$  keV and  $-33974(10)$  keV using isochronous mass spectrometry at CSRe. Referring to the  $\beta$ -delayed  $\gamma$  emissions of  $^{52}\text{Ni}$ , we identified a new excited state in  $^{52}\text{Co}$  and assigned it as the  $T = 2, J^\pi = 0^+$  isobaric analog state (IAS) of  $^{52}\text{Ni}$ . This state is  $135(17)$  keV less bound than that suggested previously based on the  $\beta$ -delayed protons of  $^{52}\text{Ni}$ . We find that the mass of this IAS together with those of the IAS's in  $^{52}\text{Fe}$ ,  $^{52}\text{Mn}$ , and  $^{52}\text{Cr}$  fit well into the Isobaric Multiplet Mass Equation. An interesting finding from this measurement is that the IAS in  $^{52}\text{Co}$  decays dominantly via  $\gamma$  transitions while proton emission is almost negligible. This phenomenon could be due to very low isospin mixing according to the large-scale shell model calculations.

*The 26th International Nuclear Physics Conference  
11-16 September, 2016  
Adelaide, Australia*

\*The work was supported by the Major State Basic Research Development Program of China (Contract No. 2013CB834401), the National Key Program for S&T Research and Development (2016YFA0400504), the NSFC grants U1232208, U1432125, 11205205, 11035007, 11235001, 11320101004, 11575007, the Chinese Academy of Sciences, and the Helmholtz-CAS Joint Research Group (HCJRG-108).

<sup>†</sup>Speaker.

## 1. Introduction

The concept of isospin was introduced by Heisenberg [1] and developed by Wigner [2] to describe the charge independence of nuclear forces. This concept is being widely used in particle and nuclear physics [3, 4]. Within the isospin formalism, a nucleus composed of  $Z$  protons and  $N$  neutrons has a fixed isospin projection of  $T_z = (N - Z)/2$ , while all states in the nucleus can have different total isospins  $T \geq |T_z|$ . In other words, states of a given  $T$  can occur in a set of isobaric nuclei with  $T_z = T, T - 1, \dots, -T$ . These states with the same  $T$  and  $J^\pi$  are called the isobaric analog states (IAS). The states with  $T = |T_z|$  are the ground states of the corresponding nuclei and the ones with  $T > |T_z|$  are excited states, except for some odd-odd  $N = Z$  nuclei [5, 6]. A set of IASs with fixed  $A$  and  $T$  are believed to have very similar structure and properties and to be energetically degenerated in the framework of isospin symmetry. This energy degeneracy is mainly altered due to the Coulomb interaction, the proton-neutron mass difference, and the charge-dependent forces of nuclear origin [7]. In an isobaric multiplet, the masses of the IASs of a given  $T$  can be described in first order approximation by the famous quadratic Isobaric Multiplet Mass Equation IMME [8, 9, 10]

$$ME(A, T, T_z) = a(A, T) + b(A, T)T_z + c(A, T)T_z^2, \quad (1.1)$$

where  $a$ ,  $b$ , and  $c$  are coefficients.

Identification of IASs and determination of their basic properties, like energies, lifetimes and decay branching ratios, has long been an important research subject. The latter is due to several motivations: (i) extracted Coulomb displacement energies between neighboring IASs constrain nuclear structure theory and allow for investigations of isospin-symmetry breaking effects of different origins (see Refs. [11, 12, 13] for reviews); (ii) a complete set of masses for any  $T \geq 1$  isobaric multiplet in the  $sd$ - or  $fp$ -shell can be used to test the validity of the IMME [14, 15, 16] as well as to extract information on the vector and tensor components of the isospin non-conserving forces [17, 18]; (iii) precise mass values of the  $T = 1$  IASs are used, in combination with the associated super-allowed  $0^+ \rightarrow 0^+$   $\beta$  decay properties, to test the Conserved Vector Current hypothesis of the electroweak interaction [19, 20], which is an active research field for more than 50-years; (iv) the analysis of the IASs provides accurate mass predictions for neutron-deficient nuclei yet inaccessible in experiments, which in turn are valuable, e.g., for modelling the astrophysical  $rp$ -process of nucleosynthesis [21, 22].

A compilation of data on the IASs throughout the nuclear chart can be found in Ref. [23]. The  $T = 2, J^\pi = 0^+$  IAS in  $^{52}\text{Co}$  was proposed in Refs. [24, 25, 26] based on the data from  $\beta$ -delayed proton decay ( $\beta$ - $p$ ) of the  $T_z = -2$  nucleus  $^{52}\text{Ni}$ . However its energy was excluded from the recent evaluation of the IASs since it significantly deviates from the value calculated with the IMME [27]. In this talk, we report on the first measurement of the masses of ground state  $^{52}\text{Co}$  and its low-lying ( $2^+$ ) isomer. Combined with data on  $\beta$ -delayed  $\gamma$ -decay ( $\beta$ - $\gamma$ ) of  $^{52}\text{Ni}$  [25, 26], this allowed us to determine the energy of the  $T = 2$  IAS in  $^{52}\text{Co}$ . We show that the IAS decays predominantly through  $\gamma$  de-excitation and thus question the conventional way of IAS assignment based on the relative intensity of proton groups [28].

## 2. Experiment and Results

The experiment was performed at the Heavy Ion Research Facility in Lanzhou (HIRFL) and Cooler Storage Ring (CSR) accelerator complex. The high-energy part of the facility consists of a main cooler-storage ring (CSRm), operating as a heavy-ion synchrotron, and an experimental ring CSRe coupled to CSRm by an in-flight fragment separator RIBLL2 [29]. Details of the experiment and data analysis can be found in Ref. [30]. In brief, a 467.91 MeV/u  $^{58}\text{Ni}^{19+}$  primary beam from the CSRm was focused onto a  $\sim 15$  mm thick beryllium target placed in front of the in-flight fragment separator RIBLL2. The reaction products from projectile fragmentation of  $^{58}\text{Ni}$  emerged from the target at relativistic energies and mostly as bare nuclei. The charge-state distributions can be estimated with a specialized CHARGE code [31]. For instance, the calculated fraction of fully-ionized atoms for Co is 99.92%. The fragments were selected and analyzed [32] by RIBLL2. A cocktail beams of 10  $\sim$  20 particles per spill were injected into the CSRe. The CSRe was tuned into the isochronous ion-optical mode [30, 33] with the transition point at  $\gamma_t = 1.4$ . The primary beam energy was selected according to the LISE++ simulations [34] such that the  $^{52}\text{Co}^{27+}$  ions had the most probable velocity with  $\gamma = \gamma_t$  at the exit of the target. Both RIBLL2 and CSRe were set to a fixed magnetic rigidity of  $B\rho = 5.8574$  Tm to allow for an optimal transmission of the  $T_z = -1$  nuclides centered on  $^{52}\text{Co}$ . In order to increase the mass resolving power, a 60 mm wide slit was introduced in the dispersive straight section of the CSRe to reduce the momentum spread of the secondary beams in the CSRe.

The revolution times of the stored ions were measured using a timing detector [35] installed inside the ring aperture. Each time an ion passed through the carbon foil of the detector, a timing signal was generated and recorded by a fast digital oscilloscope. By analyzing the timing signals the revolution time for each ion was obtained, and finally the revolution-time spectrum was created by accumulating all the events. Figure 1 shows a part of the spectrum measured in this work and zoomed in at a time window of  $608 \text{ ns} \leq t \leq 619 \text{ ns}$ . Unambiguous identification of the peaks was done in the same way as in Ref. [30] on the basis of comparison between the measured and simulated revolution time spectra. The clearly resolved ground- ( $^{52g}\text{Co}$ ) and low-lying isomeric- ( $^{52m}\text{Co}$ ) states of  $^{52}\text{Co}$  are shown in the insert.

The analysis of data was conducted according to the procedure described in [16, 30, 36, 37]. The measured revolution times of  $^{52}\text{Co}$  and its ( $2^+$ ) isomer were fitted using the un-binned maximum likelihood method. The mean revolution times of the ground and isomeric states of  $^{52}\text{Co}$  were determined to be 613.89685(5) ns and 613.89935(7) ns, respectively. The corresponding mass values were then determined via the interpolation of the mass calibration function.

The mass excesses,  $ME = (m - A \cdot u)c^2$ , are directly measured in this work to be  $ME(^{52g}\text{Co}) = -34361(8)$  keV and  $ME(^{52m}\text{Co}) = -33974(10)$  keV, respectively. These values are by 371(200) keV and 364(220) keV, respectively, lower than the extrapolated ones in the latest Atomic-Mass Evaluation (AME'12) [6]. The isomer excitation energy equals to  $E_x = 387(13)$  keV, which is very close to  $E_x = 378$  keV of the  $2^+$  isomer in the mirror nucleus  $^{52}\text{Mn}$  [38].

## 3. Identification of the T=2 IAS in $^{52}\text{Co}$

The  $\beta$ -p and  $\beta$ - $\gamma$  decay of the  $T_z = -2$  nucleus  $^{52}\text{Ni}$  was investigated in Refs. [24, 25, 26],

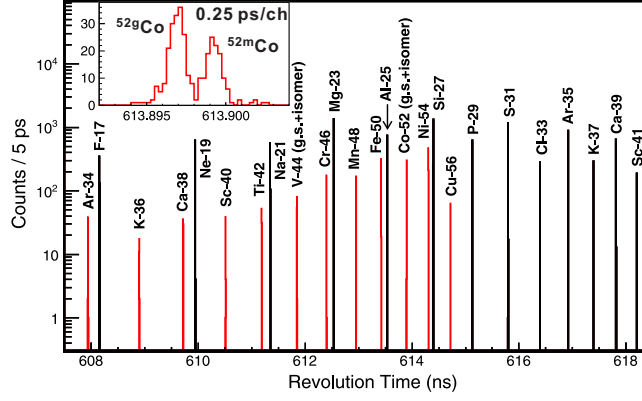


**Figure 1:** (Colour online) Part of the revolution time spectrum zoomed in at a time window of  $608 \text{ ns} \leq t \leq 619 \text{ ns}$ . The red and black peaks represent the  $T_z = -1$  and  $-1/2$  nuclei, respectively. The insert shows well-resolved peaks of the ground- and  $(2^+)$  isomeric- states of  $^{52}\text{Co}$ .

where a strong proton peak with decay energy of  $Q_p = 1352 \text{ keV}$  and a  $\gamma$  cascade of 2407- and 141-keV sequential transitions were observed. In the following we use the most recent data from Ref. [26]. As conventionally done, the strongest 1352-keV proton peak was first assigned in Ref. [24] and then adopted in Refs. [25, 26] as being due to the de-excitation of the expected IAS in  $^{52}\text{Co}$  to the ground state of  $^{51}\text{Fe}$ , thus giving the mass excess of the IAS of  $ME(^{52}\text{Co}^{\text{IAS}}) = -31561(14) \text{ keV}$ . The coincident 2407(1) keV and 141(1) keV  $\gamma$  rays de-excite the IAS feeding the  $(2^+)$  isomer in  $^{52}\text{Co}$  (see Refs. [25, 26]). Since the masses of  $^{52g,52m}\text{Co}$  have been measured in this work, the  $ME(^{52}\text{Co}^{\text{IAS}})$  could *independently* be determined to be  $ME(^{52}\text{Co}^{\text{IAS}}) = -31426(10) \text{ keV}$ . The two  $ME$  values disagree by 135(17) keV. This  $\sim 8\sigma$  deviation can not be due to experimental uncertainties and calls for a different interpretation of available data, namely that the observed 2407-keV  $\gamma$  and 1352(10)-keV proton in the decay of  $^{52}\text{Ni}$  [25, 26] are from two different excited states in  $^{52}\text{Co}$ .

We emphasize that the same experiment [26] reports  $\beta$ - $p$  and  $\beta$ - $\gamma$  data of the  $^{48}\text{Fe}$  decay. By using the proton-decay energy  $Q_p = 1018(10) \text{ keV}$  from Ref. [26] and  $ME(^{47}\text{Cr}) = -34561(7) \text{ keV}$  from Ref. [6],  $ME(^{48}\text{Mn}^{\text{IAS}}) = -26254(12) \text{ keV}$  can be deduced. The mass of  $^{48}\text{Mn}$  was also measured in our experiment. Taking our  $ME(^{48}\text{Mn}) = -29299(7) \text{ keV}$  and the corresponding  $\gamma$ -ray energies from Ref. [26], we get  $ME(^{48}\text{Mn}^{\text{IAS}}) = -26263(12) \text{ keV}$ . We see that two  $ME(^{48}\text{Mn}^{\text{IAS}})$  values from two decay channels of the IAS in  $^{48}\text{Mn}$  are in excellent agreement. This agreement supports our approach in the analysis of the  $^{52}\text{Co}$  data.

The absolute intensity of 42(10)% for the 2407-keV  $\gamma$  transition measured in  $^{52}\text{Co}$  is much stronger than the 13.7(2)% 1352(10)-keV proton emission [26]. Hence, it is reasonable to assign the former as from the IAS in  $^{52}\text{Co}$  with  $ME = -31426(10) \text{ keV}$ , and the latter as from a  $1^+$  state with  $ME = -31561(14) \text{ keV}$ , which could be the analog  $1^+$  state to the one identified in the mirror nucleus  $^{52}\text{Mn}$  [38, 39].

The assignment of the  $ME(^{52}\text{Co}^{\text{IAS}}) = -31426(10) \text{ keV}$  can further be tested by the IMME, see Eq. (1.1). A deviation to the quadratic form of the IMME can be quantified by adding a cubic term  $d \times T_z^3$ . By using the  $ME(^{52}\text{Co}^{\text{IAS}}) = -31561(14) \text{ keV}$ , Dossat *et al.* found that the  $d$ -coefficient deviates significantly from zero. They attributed this deviation to a misidentification of

one of the states assigned to this isobaric multiplet. Recently, the experimental IASs from  $T = 1/2$  to  $T = 3$  have been evaluated and the associated IMME coefficients were investigated in Ref. [27]. The assigned  $ME(^{52}\text{Co}^{\text{IAS}}) = -31561(14)$  keV in Refs. [24, 25, 26] had to be excluded from the IMME fit because the  $c$ -coefficient dramatically deviates from a smooth trend. In contrary, our  $ME(^{52}\text{Co}^{\text{IAS}}) = -31426(10)$  keV combined with known  $T = 2$  IASs in  $^{52}\text{Fe}$ ,  $^{52}\text{Mn}$ , and  $^{52}\text{Cr}$  fits well into the quadratic form of the IMME with a normalized  $\chi_n = 1.37$ . The corresponding calculated  $d$ -coefficient,  $d = 5.8(4.2)$ , is compatible with zero within  $1.4\sigma$ .

#### 4. $\beta$ -decay properties of $^{52}\text{Ni}$

Taking the newly assigned IAS in  $^{52}\text{Co}$  and the  $\beta$ - $p$  and  $\beta$ - $\gamma$  data of  $^{52}\text{Ni}$  [25, 26], we reconstructed the partial decay scheme of  $^{52}\text{Ni}$  as shown in Fig. 2. The  $J^\pi$  assignments for the levels in  $^{52}\text{Co}$  are inferred from the analogous states in the mirror nucleus  $^{52}\text{Mn}$  [39]. By using the IMME, the mass excess of  $^{52}\text{Ni}$  is predicted to be  $ME(^{52}\text{Ni}) = -22699(22)$  keV and the  $Q_{\text{EC}}$  value of  $^{52}\text{Ni}$  is thus deduced to be  $11662(23)$  keV. The main modification in the present level scheme is that we attribute the 1352-keV proton to originate from the decay of the  $1_b^+$  state rather than from the IAS. The excitation energies of the  $1_a^+$  and  $1_b^+$  states are calculated by subtracting the  $ME(^{52g}\text{Co})$  measured in this work from the  $ME$  values deduced from the  $\beta$ - $p$  data. The  $\log ft$  values are deduced [40] for each individual  $\beta$  transitions according to this partial level scheme and the  $\beta$ - $p$  and  $\beta$ - $\gamma$  intensities given in Ref. [26]. The rather small  $\log ft$  value of  $3.33(11)$  to the IAS is consistent with the super-allowed Fermi decay of  $^{52}\text{Ni}$ .

As it is usually expected in the  $sd$ - and  $fp$ -shell neutron-deficient nuclei, the newly assigned IAS should proceed via a strong 1487(14)-keV proton emission to the ground state of  $^{51}\text{Fe}$ . However, such a proton peak was not observed in the high-statistics proton spectrum in Fig. 16 of Ref. [26]. The strongest proton peak there is at 1352 keV and it does not show any visible broadening. Taking into account that the Double-Sided Silicon Strip Detector (DSSSD) used in Ref. [26] had an energy resolution of 70 keV (FWHM), two nearby proton peaks with 135 keV energy difference would clearly be separated in the  $\beta$ - $p$  spectrum of  $^{52}\text{Ni}$ . Hence, we conclude that the proton decay branch of the IAS in  $^{52}\text{Co}$  is negligibly small.

This finding has important implications on the identification of the IASs in the study of  $\beta$ -delayed charged-particle emissions [41]. It has been conventionally assumed that the IAS in a neutron-deficient nucleus decays mainly, when it is more than 1 MeV proton-unbound, via a proton emission due to a small isospin mixing [28, 41]. Consequently, the strongest proton peak is often assigned as being from the IAS of a daughter nucleus of the  $\beta$ - $p$  precursor [25, 41]. This identification may become not safe in the  $fp$ -shell nuclei, e.g., in the  $^{52}\text{Ni}$  decay, if no other information is available. By inspecting Ref. [25] we find that for several neutron-deficient  $fp$ -shell nuclei the  $\beta$ - $p$  strengths from the IASs are much weaker than the predictions of the super-allowed  $\beta^+$  feeding. Therefore it is crucial to measure  $\beta$ - $\gamma$  data in order to make a firm identification of the IAS. Indeed, such a measurement has been performed recently on  $^{53}\text{Ni}$  [42] and the  $T = 3/2$  IAS in  $^{53}\text{Co}$  was found to be  $\sim 70$  keV below the previously assigned IAS on the basis of  $\beta$ - $p$  emission data [25].

In this work we identified a new case,  $^{52}\text{Co}$ , in which the IAS decays by  $\gamma$  transition rather than by proton emission although it is  $\sim 1.5$  MeV proton-unbound. To understand this phenomenon

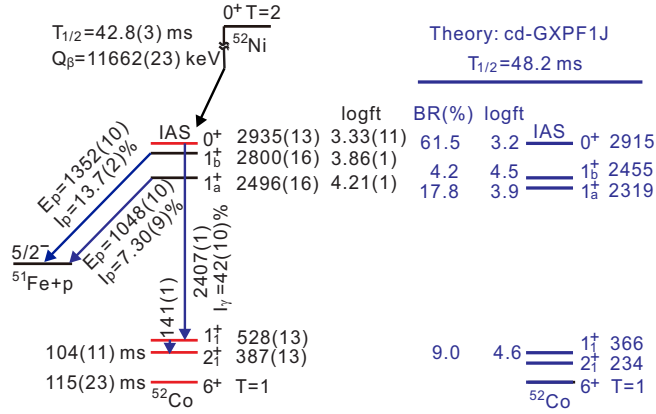


**Figure 2:** (Color online) Partial decay scheme of  $^{52}\text{Ni}$  (left) and theoretical level structure of  $^{52}\text{Co}$  (right). Excitation energies are in keV. The theoretical branching ratios ( $BR$ ) and  $\log ft$  values based on cd-GXPF1J are deduced from the *present*  $Q$  value. The red levels are deduced from the ground-state mass of  $^{52}\text{Co}$  and the  $\gamma$ -ray energies from Ref. [26]. The black levels are determined from the  $\beta$ - $p$  data.

and explore the details of the reconstructed partial decay scheme of  $^{52}\text{Ni}$ , we performed large-scale shell model calculations in the full  $fp$ -shell by using NuShellX@MSU code [43]. The isospin non-conserving (INC) Hamiltonian (hereinafter referred to as cd-GXPF1J) is constructed based on the isospin conserving Hamiltonian cd-GXPF1J [44], the Coulomb interaction, and the isovector single-particle energies (IVSPEs) [45] scaled as  $\sqrt{\hbar\omega(A)}$  [18]. A quenching factor  $q_F=0.74$  to the Gamow-Teller (GT) operator is employed to calculate the  $\beta$ -decay strength distribution. The modern GXPF1J interaction has recently been used to reproduce various experimental Gamow-Teller (GT) strengths in the region close to  $A = 52$  [39]. The calculated results are shown in the right part of Fig. 2 including the partial level structure of  $^{52}\text{Co}$ ,  $^{52}\text{Ni}$   $\beta$ -decay branching ratios,  $BR$ , and their  $\log ft$  values. Calculations agree well to the experiment. Furthermore, the theoretical half-life of 48.2 ms agrees well to the experimental one of 42.8(3) ms [6].

The proton- and  $\gamma$ -decay branches from the excited states of  $^{52}\text{Co}$  were calculated. The  $\gamma$  widths,  $\Gamma_\gamma$ , were deduced by using the effective electromagnetic operators from Ref. [46]. The total proton width can be described as  $\Gamma_p = \sum_{nlj} C^2S(nlj)\Gamma_{sp}(nlj)$ , where  $C^2S(nlj)$  is a single-particle spectroscopic factor, and  $\Gamma_{sp}$  denotes a single-particle width for the proton emission from an  $(nlj)$  quantum orbital [47]. The  $\Gamma_{sp}$  is obtained from proton scattering cross sections described by the Woods-Saxon potential [48, 49]. Two important results are obtained:

(1) Our theoretical calculations predict a super-allowed  $\beta$  transition of  $^{52}\text{Ni}$  to its IAS in  $^{52}\text{Co}$  with a branching ratio of 61.5%. Furthermore, three Gamow-Teller transitions are predicted to feed the  $1^+$  states below IAS with branching ratios of 4% through 18% (see Fig. 2). The four calculated  $\beta$ -decay branches sum to 92.5% of the total decay strength of  $^{52}\text{Ni}$ , which is in good agreement with the expected  $\beta$ -decay spectrum deduced from the  $^{52}\text{Cr}(^3\text{He},t)^{52}\text{Mn}$  charge exchange reaction [39]. Especially the relative strengths of the three Gamow-Teller transitions have been well reproduced.

(2) The calculations show that the total proton width of the IAS,  $\Gamma_p^{\text{IAS}}$ , is 0.0001 eV, which is three orders of magnitude smaller than  $\Gamma_\gamma^{\text{IAS}} = 0.25$  eV. This indicates that the IAS in  $^{52}\text{Co}$  decays predominantly via  $\gamma$  transitions. The proton emission should be orders of magnitude weaker than the  $\gamma$  transitions and is thus unlikely to be observed experimentally. In fact, the  $\beta$ - $p$  emission from

IAS is isospin forbidden, and the observation of such a proton emission is usually attributed to the isospin mixing of the IAS with the nearby  $T = 1, J^\pi = 0^+$  states. In our shell model calculations, the closest  $0^+$  state is predicted to be 168 keV below the IAS and the isospin mixing imposed from this  $0^+$  to the IAS is calculated to be merely 0.23%. The small isospin mixing indicates that no observable proton emission from the IAS is expected, which is consistent with our re-constructed decay scheme of  $^{52}\text{Ni}$  (see Fig. 2). Concerning the  $1_a^+$  and  $1_b^+$  states, the total proton widths are 0.6 eV and 37.8 eV, respectively, which are orders of magnitude larger than the  $\gamma$  widths of  $\Gamma_\gamma(1_a^+) = 0.05$  eV and  $\Gamma_\gamma(1_b^+) = 0.04$  eV, respectively. This is again consistent with experiment that both  $1^+$  states de-excite predominantly via proton emission and the  $\gamma$  transitions were too weak to be observed [25, 26].

Although our shell model calculations provide an overall consistent interpretation of all available data on the  $\beta$ -decay of  $^{52}\text{Ni}$ , there are, however, three remaining open questions: (1) the measured intensity of 7.3% for the 1048-keV proton is much weaker than the predicted  $\beta$  feeding of 17.8%; (2) the intensity of 13.7% for the 1352 keV proton emission is much higher than the predicted  $\beta$  feeding of 4.2%; (3) the intensity of 42% for the 2407-keV  $\gamma$  transition is lower than the predicted Fermi  $\beta$  feeding of 61.5%.

The first point may be caused by the un-observed  $\gamma$  rays or protons de-exciting the  $1_a^+$  level. The last two points may be interpreted, at least qualitatively, by assuming an  $\text{IAS} \rightarrow 1_b^+$  transition via  $\gamma$  and internal electron conversion. Such an exotic  $\beta$ -delayed  $\gamma$ - $p$  decay has been observed in its neighboring nucleus  $^{56}\text{Zn}$  [50], although the comparable  $\text{IAS} \rightarrow 1_b^+$  decay branching in  $^{52}\text{Co}$  can not be predicted in our calculations.

The questions raised above vitalize us to propose an alternative scenario based on the hypothesis that there would exist a low-lying spherical state in  $^{51}\text{Fe}$  to which the IAS of  $^{52}\text{Co}$  may decay via proton emission. On the one hand, the ground-state of  $^{52}\text{Ni}$  is thought to be spherical due to its semi-magic character. Hence the IAS in  $^{52}\text{Co}$  should also be spherical according to the isospin symmetry. On the other hand, the rotation-like bands have been observed in  $^{50,51,52}\text{Fe}$  [51, 52, 53] indicating that the ground states of these isotopes are slightly deformed. Thus, the proton emission from the spherical  $T = 2$  IAS in  $^{52}\text{Co}$  to the  $T = 1/2$  deformed states in  $^{51}\text{Fe}$  are hindered not only by the isospin selection rules but also by the shape changes between the final and initial nuclear states, causing the proton emission from IAS to be less likely. However, if a shape coexistence in  $^{51}\text{Fe}$  is considered, it is possible that the soft nucleus  $^{51}\text{Fe}$  has in its Potential Energy Surface (PES) a second minimum with a nearly-spherical shape. To check this, we have performed PES calculations [54] for  $^{51}\text{Fe}$ . Apart from the deformed minimum at  $(\beta_2, \gamma) = (0.16, -10^\circ)$  corresponding to the  $5/2^-$  ground state, there exists a shallow – nearly-spherical – minimum  $\sim 200$  keV above the deformed one. If such a spherical minimum exists in  $^{51}\text{Fe}$ , one may attribute the 1352-keV protons, or part of them, to be originated from the decay of the IAS to the states in the second minimum of  $^{51}\text{Fe}$ . Consequently, the intensity imbalances raised in the questions above could – at least partly – be solved.

## 5. Conclusions

In conclusion,  $^{58}\text{Ni}$  projectile fragments were addressed by the isochronous mass spectrometry at HIRFL-CSR. Precision mass excess values for  $^{52g}\text{Co}$  and its low-lying ( $2^+$ ) isomer have been

precisely measured for the first time. Combining our new results with the literature  $\beta$ - $\gamma$  measurements of  $^{52}\text{Ni}$ , the energy of the  $T = 2$  isobaric analog state in  $^{52}\text{Co}$  was determined to be 135 keV higher than previously assumed on the basis of the  $\beta$ - $p$  data from the  $^{52}\text{Ni}$  decay studies. With this new IAS assignment, the mass excesses of the four members of the  $A = 52$ ,  $T = 2$  isobaric multiplet are found to be consistent with the quadratic form of the IMME. Furthermore, a remarkably different decay scheme of  $^{52}\text{Ni}$  could be constructed, in which the proton group with the highest relative intensity [25, 26] corresponds to the decay from the  $1^+$  excited state in  $^{52}\text{Co}$  and *not* from the  $0^+$ ,  $T = 2$  IAS state. This finding has important implications on the identification of the IASs from  $\beta$ -delayed charged-particle emission studies. The newly determined level scheme of  $^{52}\text{Co}$  is consistent with its mirror nucleus  $^{52}\text{Mn}$  and can well be reproduced by large-scale shell model calculations using an isospin non-conserving Hamiltonian. Our theoretical calculations indicate that the isospin mixing in the  $0^+$ ,  $T = 2$  state in  $^{52}\text{Co}$  is extremely low, thus leading to a negligibly small proton emission from this state. An alternative scenario based on a possible shape coexistence is proposed to account for the remaining intensity imbalances observed between experiment and shell model calculations. Further experiments aiming at comprehensive studies of this interesting phenomenon are required.

## References

- [1] W. Heisenberg, *Z. Phys.* **77**, 1 (1932).
- [2] E. P. Wigner, *Phys. Rev.* **51**, 106 (1937).
- [3] G. A. Miller, A. K. Opper, and E. J. Stephenson, *Ann. Rev. Nucl. Part. Sci.* **56**, 253 (2006).
- [4] *Isospin in Nuclear Physics*, edited by D. H. Wilkinson (North-Holland, Amsterdam, 1969).
- [5] J. Jänecke, T. W. O'Donnell and V. I. Goldanskii, *Phys. Rev. C* **66**, 024327 (2002).
- [6] M. Wang *et al.*, *Chin. Phys. C* **36**, 1603 (2012), and G. Audi *et al.*, *Chin. Phys. C* **36**, 1157 (2012).
- [7] M. A. Bentley and S. M. Lenzi, *Prog. Part. Nucl. Phys.* **59**, 497 (2007).
- [8] E. P. Wigner, in *Proc. of the R. A. Welch Foundation Conf. on Chemical Research, Houston*, edited by W. O. Milligan (R. A. Welch Foundation, Houston, 1957), Vol. 1.
- [9] S. Weinberg and S. B. Treiman, *Phys. Rev.* **116**, 465 (1959).
- [10] W. Benenson and E. Kashy, *Rev. Mod. Phys.* **51**, 527 (1979).
- [11] J. A. Nolen and J. P. Schiffer, *Ann. Rev. Nucl. Sci.* **19**, 471 (1969).
- [12] S. Shlomo, *Rep. Prog. Phys.* **41**, 958 (1978)
- [13] M. A. Bentley and S. M. Lenzi, *Prog. Part. Nucl. Phys.* **50**, 497 (2007)
- [14] K. Blaum *et al.*, *Phys. Rev. Lett.* **91**, 260801 (2003).
- [15] A. T. Gallant *et al.*, *Phys. Rev. Lett.* **113**, 082501 (2014) .
- [16] Y. H. Zhang *et al.*, *Phys. Rev. Lett.* **107**, 102501 (2012).
- [17] W. E. Ormand and B. A. Brown, *Nucl. Phys. A* **491**, 1 (1989).
- [18] Y. H. Lam, N. A. Smirnova, and E. Caurier, *Phys. Rev. C* **87**, 054304 (2013).

- [19] J. C. Hardy and I. S. Towner, Phys. Rev. Lett. **94**, 092502 (2005).
- [20] J. C. Hardy and I. S. Towner, Phys. Rev. C **91**, 025501 (2015).
- [21] H. Schatz and K. E. Rehm, Nucl. Phys. **A777**, 601 (2006).
- [22] A. Parikh *et al.*, Phys. Rev. C **79**, 045802 (2009).
- [23] M. S. Antony, A. Pape, and J. Britz, At. Data Nucl. Data Tables **66**, 1 (1997).
- [24] L. Faux *et al.*, Phys. Rev. C **49**, 2440 (1994).
- [25] C. Dossat, *et al.*, Nucl. Phys. **A792**, 18(2007).
- [26] S. E. A. Orrigo *et al.*, Phys. Rev. C **93**, 044336 (2016).
- [27] M. MacCormick and G. Audi, Nucl. Phys. **A915**, 61 (2014).
- [28] J. Cerny and J. C. Hardy, Ann. Rev. Nucl. Part. Sci. **27**, 333 (1977).
- [29] J. W. Xia *et al.*, Nucl. Instrum. Methods Phys. Res., Sect. A **488**, 11 (2002).
- [30] X. L. Tu *et al.*, Nucl. Instrum. Methods Phys. Res., Sect. A **654**, 213 (2011).
- [31] C. Scheidenberger *et al.*, Nucl. Instrum. Methods Phys. Res., Sect. B **142**, 441 (1998).
- [32] H. Geissel *et al.*, Nucl. Instrum. Methods Phys. Res., Sect. B **70**, 286 (1992).
- [33] M. Hausmann *et al.*, Nucl. Instrum. Methods Phys. Res., Sect. A **446**, 569 (2000).
- [34] O. B. Tarasov and D. Bazin, Nucl. Instrum. Methods Phys. Res., Sect. B **266**, 4657 (2008).
- [35] B. Mei, *et al.*, Nucl. Instrum. Methods Phys. Res., Sect. A **624**, 109 (2010).
- [36] X. L. Tu, *et al.*, Phys. Rev. Lett. **106**, 112501 (2011).
- [37] P. Shuai, *et al.*, Phys. Lett. B **735**, 327 (2014).
- [38] R. M. DelVecchio, Phys. Rev. C **7**, 677 (1973).
- [39] Y. Fujita *et al.*, Acta Phys. Pol. B **46**, 657 (2015).
- [40] <http://www.nndc.bnl.gov/logft/>.
- [41] B. Blank and M. J. G. Borge, Prog. Part. Nucl. Phys. **60**, 403 (2008).
- [42] J. Su *et al.*, Phys. Lett. **B756**, 323 (2016).
- [43] B. A. Brown and W. D. M. Rae, Nucl. Data Sheets **120**, 115 (2014).
- [44] M. Honma *et al.*, J. Phys. Conf. Ser. **20**, 7 (2005).
- [45] W. E. Ormand and B. A. Brown, Nucl. Phys. **A440**, 274 (1985).
- [46] M. Honma *et al.*, Phys. Rev. C **69**, 034335 (2004).
- [47] M. H. Macfarlane and J. B. French, Rev. Mod. Phys. **32**, 567 (1960).
- [48] Y. H. Lam *et al.*, Astrophys. J. **818**, 78 (2016).
- [49] B. A. Brown (WSPOT), <ftp://www.nsl.mscl.msu.edu/~brown/reaction-codes/home.html>
- [50] S. E. A. Orrigo *et al.*, Phys. Rev. Lett. **112**, 222501 (2014).
- [51] S. M. Lenzi *et al.*, Phys. Rev. Lett. **87**, 122501 (2001).
- [52] M. A. Bentley *et al.*, Phys. Rev. C **62**, 051303(R) (2000).
- [53] C. A. Ur *et al.*, Phys. Rev. C **58**, 3163 (1998).
- [54] F. R. Xu, W. Satula, and R. Wyss, Nucl. Phys. **A669**, 119 (2000).